**Atmospheric
Chemistry
and Physics**

Variability and budget of CO_2 in Europe: analysis of the CAATER airborne campaigns – Part 1: Observed variability

I. Xueref-Remy[1], **C. Messager**[1], **D. Filippi**[2], **M. Pastel**[3], **P. Nedelec**[4], **M. Ramonet**[1], **J. D. Paris**[1], **and P. Ciais**[1]

[1]Laboratoire des Sciences du Climat et de l'Environnement (LSCE)/Institut Pierre Simon Laplace, UMR1572, CEA Orme des Merisiers, 91191 Gif-sur-Yvette CEDEX, France
[2]Sextant Technology Ltd, 116 Wilton Road, Wellington 6012, New Zealand
[3]Laboratoire Atmosphères, Milieux, Observations Spatiales (LATMOS)/Institut Pierre Simon Laplace (CNRS,UVSQ), 78280 Guyancourt, France
[4]Laboratoire d'Aérologie (LA), 14 avenue Edouard Belin, 31400 Toulouse, France

Abstract. Atmospheric airborne measurements of CO_2 are very well suited for estimating the time-varying distribution of carbon sources and sinks at the regional scale due to the large geographical area covered over a short time. We present here an analysis of two cross-European airborne campaigns carried out on 23–26 May 2001 (CAATER-1) and 2–3 October 2002 (CAATER-2) over Western Europe. The area covered during CAATER-1 and CAATER-2 was 4° W to 14° E long; 44° N to 52° N lat and 1° E to 17° E long; 46° N to 52° N lat respectively. High precision in situ CO_2, CO and Radon 222 measurements were recorded. Flask samples were collected during both campaigns to cross-validate the in situ data. During CAATER-1 and CAATER-2, the mean CO_2 concentration was 370.1 ± 4.0 (1-σ standard deviation) ppm and 371.7 ± 5.0 (1-σ) ppm respectively. A HYS-PLIT back-trajectories analysis shows that during CAATER 1, northwesterly winds prevailed. In the planetary boundary layer (PBL) air masses became contaminated over Benelux and Western Germany by emissions from these highly urbanized areas, reaching about 380 ppm. Air masses passing over rural areas were depleted in CO_2 because of the photosynthesis activity of the vegetation, with observations as low as 355 ppm. During CAATER-2, the back-trajectory analysis showed that air masses were distributed among the 4 sectors. Air masses were enriched in CO_2 and CO over anthropogenic emission spots in Germany but also in Poland, as these countries have part of the most CO_2-emitting coal-based plants in Europe. Simultaneous measurements of in situ CO_2 and CO combined with back-trajectories helped us to distinguish between fossil fuel emissions and other CO_2 sources. The $\Delta CO/\Delta CO_2$ ratios ($R^2 = 0.33$ to 0.88, slopes = 2.42 to 10.37), calculated for anthropogenic-influenced air masses over different countries/regions matched national inventories quite well, showing that airborne measurements can help to identify the origin of fossil fuel emissions in the PBL even when distanced by several days/hundreds of kms from their sources. We have compared airborne CO_2 observations to nearby ground station measurements and thereby, confirmed that measurements taken in the lower few meters of the PBL (low-level ground stations) are representative of the local scale, while those located in the free troposphere (FT) (moutain stations) are representative of atmospheric CO_2 regionally on a scale of a few hundred kilometers. Stations located several 100 km away from each other differ from a few ppm in their measurements indicating the existence of a gradient within the free troposphere. Observations at stations located on top of small mountains may match the airborne data if the sampled air comes from the FT rather than coming up from the valley. Finally, the analysis of the CO_2 vertical variability conducted on the 14 profiles recorded in each campaign shows a variability at least 5 to 8 times higher in the PBL (the 1-σ standard deviation associated to the CO_2 mean of all profiles within the PBL is 4.0 ppm and 5.7 ppm for CAATER-1 and CAATER-2, respectively) than in the FT (within the FT, 1-σ is 0.5 ppm and 1.1 ppm for CAATER-1 and CAATER-2, respectively). The CO_2 jump between the PBL and the FT equals 3.7 ppm for the first campaign and -0.3 ppm for the second campaign.

A very striking zonal CO_2 gradient of about 11 ppm was observed in the mid-PBL during CAATER-2, with higher concentrations in the west than in the east. This gradient may originate from differences in atmospheric mixing, ground emission rates or Autumn's earlier start in the west. More airborne campaigns are currently under analysis in the framework of the CARBOEUROPE-IP project to better assess the likelihood of these different hypotheses. In a companion paper (Xueref-Remy et al., 2011, Part 2), a comparison of vertical profiles from observations and several modeling frameworks was conducted for both campaigns.

1   Introduction

Atmospheric greenhouse gas (GHG) concentrations have been increasing since the pre-industrial era, due to human activities such as the combustion of fossil fuel compounds and deforestation. The most significant growth has been in the presence of CO_2, its atmospheric concentration having increased by more than 30% during the last 150 yr. Political efforts have been made through the United Nations Framework Convention on Climate Change to stabilize atmospheric CO_2 concentration levels. Such efforts require independent verification of anthropogenic and natural fluxes on a regional scale, a task which represent a huge scientific and political challenge (Intergovernmental Panel on Climate Change, 2007).

The atmosphere is a strong integrator of CO_2 surface sources and sinks. Observations can thus be used to quantify surface fluxes over relatively large scales by matching them with modelled field simulations from transport models. This method, known as inverse modelling, is the approach most used to quantify CO_2 fluxes at regional or global scales. However, the flux partition, especially at the regional scale (100–1000 km) is still poorly understood. Indeed for Europe (based on data from 1992–1996), Gurney et al. (2003) have compared 16 inverse models: all indicate that Europe is a sink for CO_2 but they show very large differences, with a mean annual flux of 0.6 GtC yr^{-1} and a standard deviation of ± 0.4 GtC yr^{-1} i.e. 66% of the mean.

Briefly, these large differences originate for several reasons. Firstly, most of the studies are based on measurements done on remote and marine sites, far from where terrestrial fluxes are taking place: there is a lack of measurements over the continents to constrain flux calculations by inverse modelling (Geels et al., 2007). Secondly, models have difficulties in representing atmospheric transport in the continental planetary boundary layer (PBL) (Gerbig et al., 2003). Several intercomparison studies have been undertaken to make progress in the modeling of the fluxes and especially on a seasonal scale (e.g. Gurney et al., 2004; Baker et al., 2006; Law et al., 2008; Patra et al., 2008; Carouge et al., 2010a, b).

Globally at this level, reducing inverse modelling uncertainties requires a better characterization of atmospheric CO_2 vertical and horizontal variability through in situ observations. Over the past 10 yr, the atmospheric CO_2 global monitoring network has been largely used to retrieve large scale distribution of sources and sinks at the surface. Recent studies have demonstrated the need for more data over the continental region in order to make feasible robust estimations of the biospheric contribution to the regional carbon budget. Stephens et al. (2007) have highlighted the need for in situ vertical observations to better constrain CO_2 fluxes. Indeed, because of the large geographical area they can span within a short time, airborne measurements are very well suited to studying atmospheric CO_2 variability on a regional scale, vertically and horizontally, and, in particular, can give crucial information on the gradients between the PBL and the free troposphere (FT). Over Europe, airborne campaigns conducted in the boundary layer are very limited as resumed in Geels et al. (2007). The Co-ordinated Access to Aircraft for Transnational Environmental Research (CAATER-1 and CAATER-2), an European initiative, has given us the opportunity to perform two intensive airborne campaigns over Western Europe in May 2001 and October 2002.

The aims of these campaigns were: (1) to validate a new airborne in situ CO_2 analyzer; (2) to characterize CO_2 variability in the low troposphere above Western Europe; (3) to evaluate the contributions of anthropogenic and biospheric fluxes to this variability; (4) to assess the representativeness of ground stations; and (5) to better characterize the gradients of CO_2 between the PBL and the FT.

In this paper, we show the results of these campaigns conducted in the low troposphere (<4000 m) aboard the Falcon 20 of the Deutsches Zentrum für Luft und Raumfahrt (Oberpfaffenhofen Germany). During this experiment the Falcon was equipped with a continuous CO_2 analyser (CONDOR), a continuous CO analyser (MOZAIC CO analyser, Laboratoire d'Aérologie, France) which was used as a combustion tracer and a sequential Radon 222 analyser (AVIRAD) which was used as a tracer of continental air masses.

The conditions of the campaigns and the instrumentation deployed are presented in Sect. 2. In Sect. 3, we conduct an analysis of air mass origins using back-trajectories. In Sect. 4, we analyse the contribution of anthropogenic emissions to CO_2 variability using CO data. In Sect. 5, we assess the representativeness of ground station measurements using aircraft observations. Finally Sect. 6 focuses on CO_2 vertical variability, especially on characterizing CO_2 gradients between the PBL and the FT in function of the air mass origins. In a companion paper (Xueref-Remy et al., 2011, Part 2), we conduct a comparison between observations and models: firstly to assess the capability of a global model versus a mesoscale model to reproduce the observed gradients, incorporating also several biospheric fluxes, and secondly, to present a comparison between model-based fluxes obtained using a new method coupling backplumes
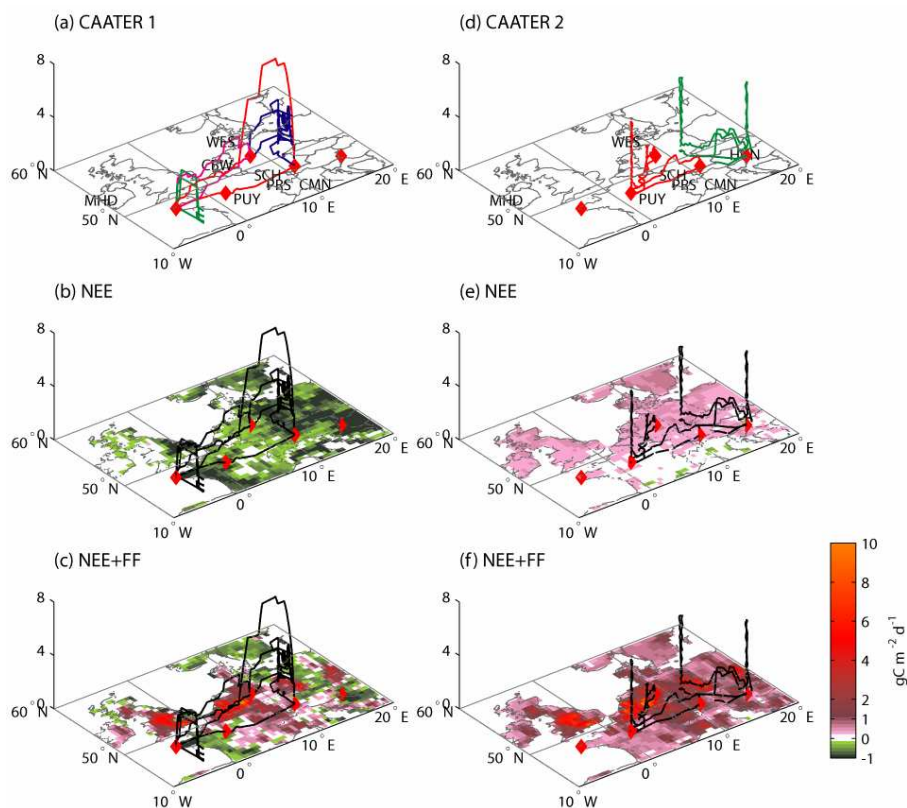
Fig. 1. Averaged flux maps (for the days of the campaigns) and flight patterns (red: 1st day, green: 2nd day, pink: 3rd day, blue: 4th day of the campaigns) according to latitude, longitude and altitude (in km). Net Ecosystem Exchange (NEE) fluxes are from ORCHIDEE and fossil fuel (FF) fluxes from Andres et al. (1996) (left: CAATER-1, right: CAATER-2). Oceanic fluxes are from Takahashi et al. (1999) and are almost zero therefore do not appear in the figure.

and a priori fluxes, and observation-based fluxes calculated with the Radon method (Schmidt et al., 2003).

2 Description of the campaigns and of instrumentation

2.1 The CAATER campaigns

The CAATER aircraft measurement (Co-ordinated Access to Aircraft for Transnational Environmental Research) programme is coordinated by the German DLR, French INSU/CNRS and Météo-France, and by the UK Met Office. The programme was funded between 2000 and 2003 by the European Commission to provide research aircraft facilities for pilot projects and new studies. The objective of the CAATER Carbon Dioxide pilot project detailed in this study is to measure the vertical and horizontal variability of CO_2 over Western Europe during two contrasted seasons. We used the DLR-Falcon 20 jet aircraft (http://www.dlr.de/fb/en/desktopdefault.aspx/tabid-3714/5789_read-8405/) equipped with (1) a CO continuous infra-red analyzer, (2) a CO_2 non dispersive infra-red gas analyzer, (3) a 222Rn sequential sampler instrument, (4) a flask sampling unit and (5) stan-

dard meteological parameter sensors (i.e., pressure, temperature, horizontal and vertical windspeeds, dewpoint temperature, absolute and relative humidities, virtual temperature and virtual potential temperature).

Two airborne campaigns were carried out in May 2001 and in October 2002, here called CAATER-1 and CAATER-2. The two flight routes are different, but they both extend across a domain of roughly 20° in longitude between Western France and West Hungary. The Falcon-20 flights for each campaign are shown in Fig. 1. The CAATER-1 campaign consisted of 5 flights for a total of 14 h during 23–26 May 2001, and the CAATER-2 campaign consisted of 3 flights for a total of 8 h during 2–3 October 2002 (Tables 1 and 2). Vertical CO_2 profiles and in the case of CAATER-2 also CO and 222-Rn, were collected between the ground and 4000 m alt during each campaign. We have 14 profiles in total for each campaign.

The paper also uses a dataset from different in situ sampling sites described in Table 3. These data will be used in Sect. 5 to assess the stations footprint by comparing them to the CAATER measurements.

Table 1. Airport acronyms and geographical information.

Code	Name	Country	Latitude	Longitude	Altitude (m a.s.l.*)
BZH	Brest	France	48°26′ N	04°25′ W	99
OBP	Oberpfaffenhofen	Germany	48°05′ N	11°17′ E	593
ORL	Orleans	France	47°53′ N	02°10′ E	120
PDB	Paderborn	Germany	51°36′ N	08°37′ E	213
SOB	Sarmellek	Hungary	46°42′ N	17°06′ E	408

* m a.s.l. = meters above sea level.

Table 2. Flight information for the CAATER 1 and CAATER 2 campaigns.

Date	Time range (hh:mm UTC)	Flight pattern	Flight number
23 May 2001	12:12–14:43	OBP – BZH	1
24 May 2001	15:03–17:50	Atlantic, south of BZH	2
25 May 2001	11:26–13:43	BZH – PDB	3
26 May 2001	08:56–15:46	PDB – OBP	4
2 October 2002	08:48–11:10	OBP – ORL	5
2 October 2002	11:10–13:16	ORL – PDB	6
3 October 2002	10:02–12:20	PDB* – SOB	7
3 October 2002	14:19–15:52	SOB – OBP	8

* No data available between PDB and THU.

Table 3. Ground station acronyms and geographical information.

Site	Name	Country	Latitude	Longitude	Ground altitude (m a.s.l.[a])	Type of station (m.a.g.l)[b]
CBW	Cabauw	Holland	51°58′ N	04°55′ E	−0.7	Tower (213 m)
CMN	Monte Cimone	Italy	44°11′ N	10°42′ E	2165	Surface (mountain top)
HUN	Hegyhatsal	Hungary	46°57′ N	16°39′ E	248	Tower (115 m)
MHD	Mace Head	Ireland	53°19′ N	09°53′ W	26	Surface
PRS	Plateau Rosa	Italy	45°56′ N	07°42′ E	3480	Surface (mountain top)
PUY	Puy-de-Dome	France	45°45′ N	03°00′ E	1465	Surface (mountain top)
SCH	Schauinsland	Germany	47°55′ N	07°55′ E	1205	Surface (mountain top)
WES	Westerland	Germany	54°56′ N	08°19′ E	12	Surface

[a] m a.s.l. = meters above sea level;

[b] m a.g.l. = meters above ground level.

2.2 CO_2 surface fluxes conditions

Because the focus of this study is to analyze the variability of CO_2 across Western Europe, it is important to understand the underlying fluxes, which we provide in this section. Figure 1 shows the average CO_2 flux maps over Western Europe during the sampling interval of each campaign. The net CO_2 flux is the sum of fossil fuel CO_2 emissions and of the Net Ecosystem Exchange flux, which can be positive (source) or negative (sink) depending upon the vegetation status. The Normalized Difference Vegetation Index (NDVI) provided by the SPOT VGT-4 satellite system reveals a higher photosynthetic activity in May than in October (see Appendix A), but vegetation index is not easy to translate into a CO_2 source/sink map. We show in Fig. 1, overlaid with the campaign flights, the three CO_2 continental flux components, i.e.: the Net Ecosystem Exchange (NEE) fluxes given by the process-based ecosystem model ORCHIDEE (Krinner et al., 2005) also described in the companion paper (Xueref-Remy et al., 2011, Part 2) with a spatial resolution of 0.35°×0.35° forced by synoptic weather data with a 3 h resolution averaged on the days of the campaign (the diurnal cycle thus being smoothed); annual fossil fuel (FF) emission maps with a spatial resolution of 1°×1° from

Andres et al. (1996) updated to the year of each campaign; and oceanic fluxes from Takahashi et al. (1999, 2002). As oceanic fluxes are negligible compared to NEE and fossil fuel fluxes, they do not appear in the maps. These maps show that for this period in May 2001, Europe was mainly acting as a CO$_2$ sink (reaching about $-1\,\mathrm{gC\,m^{-2}\,day^{-1}}$) while in early October 2002 it was acting more like a source of CO$_2$ north of 47° N (about $1\,\mathrm{gC\,m^{-2}\,day^{-1}}$) and a tiny sink south of 45° N (about $0.4\,\mathrm{gC\,m^{-2}\,day^{-1}}$). Largest fossil fuel emissions occur from the London megacity area, Benelux, Ruhr, the Berlin metropolitan area and the Warsaw city regions. The most emitting coal-fed power plants (the so-called "dirty thirty" identified by the WWF: http://www.panda.org/what_we_do/knowledge_centres/climate_change/problems/cause/coal/dirty_30/) are located here and represent 10% of European CO$_2$ emissions.

2.3 Synoptic weather conditions

Synoptic weather conditions encountered during both campaigns are shown in Fig. 2 (http://weather.ou.edu/~cgodfrey/reanalysis/).

During CAATER 1, the synoptic situation was mainly anti-cyclonic, as shown by mean sea level pressure and 850 hPa wind maps. Note that 850 hPa represents the mean aircraft altitude during the campaign (1457 m above sea level). No major cloud system was present over Europe during the campaign. During 23–24 May 2001 winds from the north-east prevailed over the campaign domain in Northern France, established around a high-pressure system located over the British Isles. On 25 May 2001, this high-pressure moved towards southern Scandinavia and north-easterly winds continued to prevail.

During CAATER 2, dry conditions were encountered, apart from 3 October 2002 when a few showers occured over Thüringen, in Eastern Germany. By 2 October 2002, a small high-pressure system over Norway induced airflow from the north into the aircraft route over Southern Germany. But another high-pressure placed over the Balkans region creates a second flow from Southern Europe into the aircraft route over France. We thus expect a very significant change in air mass origins at the boundary between these two different flow regimes. On 3 October 2002, two high-pressure systems were observed, west and east of the aircraft route, over France and Greece. This situation gives rise to complex wind patterns, as further evidenced from the back-trajectory analysis in Sect. 3.

2.4 Instrumentation

2.4.1 In situ continuous CO$_2$ measurements

In addition to standard meteorological parameters (wind, relative humidity, temperature, pressure) with a 1-Hz acquisition, the CO$_2$ concentrations were measured with a contin-
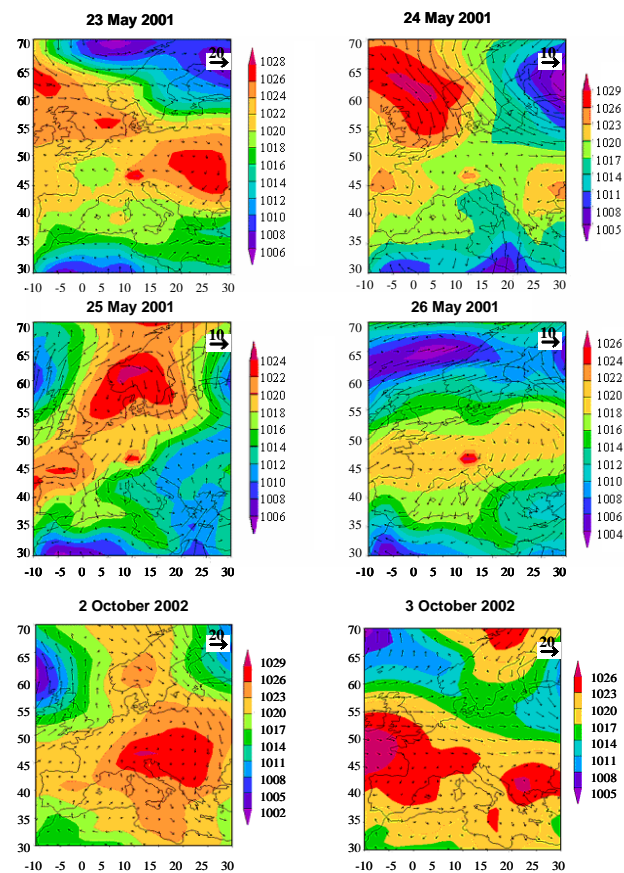

Fig. 2. Meteorological maps showing mean sea-level pressure (in hPa) and wind speed (in m s^{-1}) at 850 hPa for each day of the CAATER campaigns at 12:00:00 h UTC (http://weather.ou.edu/~cgodfrey/reanalysis/). Latitude (vertical scale) is given in ° N and longitude (horizontal scale) in ° E.

uous NDIR airborne analyzer developed at LSCE (Fig. 3). This instrument is based on a commercial sensor Li-COR 6262 with a fast response detector (1 Hz acquisition), with temperature, pressure and flow rates of air being regulated at constant values (Table 4). Outside air was pumped and dried by a magnesium perchlorate cartridge before being analyzed. More details can be found in Filippi et al. (2002).

Airborne CO$_2$ measurements are useful for carbon cycle studies (inversions) if they have a precision better than 0.5 ppm (Gloor et al., 2000). Frequent calibrations (every 30 min) give an instantaneous precision of 0.1 ppm, but slow instrument drifts due to changes in surrounding physical parameters such as pressure and temperature require frequent calibrations during flights. We used two calibration gases in high-pressure cylinders of 2 l, with concentrations in the NOAA X-93 scale of 365.92 ± 0.05 ppm (Low) and 401.29 ± 0.05 ppm (High). Each standard is passed through the analyzer for 3 min, and only the last minute of acquisition is retained to compute the calibration curve and calculate outside air CO$_2$. Given the limited volume of each

Table 4. Characteristics of the CO$_2$ and CO analyzers.

Parameter	CO$_2$ analyzer (CONDOR)	CO analyzer
Precision	≤ 0.20 ppm for 1 s	± 5 ppbv for 30 s
Sampling frequency	1 Hz	0.03 Hz
Power supply	18-32VDC/15A max	24V/10A max
Cells pressure	1080 hPa	2532 hPa
Flow rates	50 sccm (Reference cell) 400 sccm (Sample cell)	4000 sccm
Temperature	35 °C	30 °C
Calibrations	1 calibration (6 mn) every 30 mn	Before and after each campaign
Volume	$95 \times 55 \times 40$ cm^3	$60 \times 31 \times 43$ cm^3
Weight	80 kg	45 kg
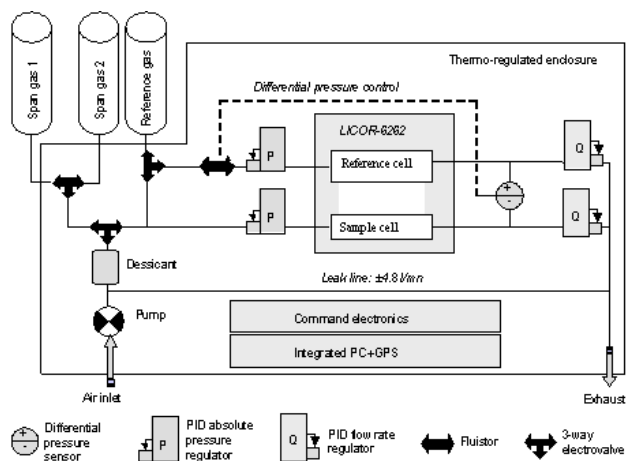
Fig. 3. Schematic of the CONDOR analyzer.

cylinder, the time taken for calibration and the sought precision, an optimal compromise had to be found. We carried out ≈ 30 calibrations during each campaign. The average stability (1-σ std. deviation on 1-Hz data) was 0.03 ppm during the last minute of each calibration passage. To compute the instrument accuracy, each calibration gas was treated as an unknown target. The difference between the true and the measured target value is 0.10 ppm for the high standard and 0.08 ppm for the low one. Also, we found that, even when using one single calibration result before each flight, the instrument accuracy is still greater than 0.20 ppm.

2.4.2 Flasks analysis

To independently assess the instruments accuracy, about 50 1-l glass flasks were sampled during each campaign. After 5 min of flushing, the sampled air was compressed at 1 bar above atmospheric pressure to avoid any contamination due to leakage. The CO$_2$ concentration was measured by gas chromatography at LSCE with a precision <0.10 ppm (Pépin et al., 2001), each flask being measured twice. A flask con-

centration was systematically rejected if the two measurements differed by more than 0.10 ppm (3.2% of the samples). The mean difference between the in situ NDIR and the flasks was less than 0.20 ppm for both campaigns (see Appendix B, Fig. B1).

2.4.3 In situ continuous CO measurements

The CO analyser is the same as the one developed for routine measurements onboard passenger aircrafts for the MOZAIC program (http://mozaic.aero.obs-mip.fr/web/). CO was only measured during CAATER-2 and its characteristics are summarized in Table 4. This analyser described in Nedelec et al. (2003) is a fully automated instrument designed to reach an accuracy of 5%. It is based on the commercial IR correlation gas analyser Model48C produced by Thermo Environment Instruments [TEI, USA]. It is a Gas Filter Correlation instrument based on the principle of infra-red absorption by the 4.67 μm fundamental vibration-rotation band of CO. Radiation from an infrared source is chopped and passed through a gas filter which alternates between CO and N$_2$. The radiation then passes through a narrow band pass filter and a multiple optical pass sample cell where absorption by the sample gas occurs. The IR radiation exits the sample cell and falls on a lead-selenium solid state IR detector. Other gases do not cause modulation of the detector signal since they absorb the reference and measure beams equally. Thus, the Gas Filter Correlation System responds specifically to CO. The Model 48CTL is also qualified by US EPA designated Method (EQSA-0486-060). The specification of the commercial instrument is 10 ppbv CO for 300 s integration time. Major improvements have been brought by Nédélec et al. (2003): periodic accurate zero measurements, new IR detector with better cooling and temperature regulation, pressure increase and regulation in the absorption cell, increased flow rate to 4 l min^{-1}, water vapor trap, and ozone filter. The specifications achieved for 30 s integration time (response time of the instrument) are a precision of ± 5 ppbv CO with a minimum detectable of 10 ppbv of CO. The instrument was calibrated before and after the campaign with

a traceable CO cylinder from the National Institute of Standards and Technology in Boulder, Colorado, USA.

3 Origin of sampled air masses

3.1 Mean CO_2, CO concentrations and back-trajectories

The CO_2 distribution observed over the European continent results from the mixing of oceanic background air with continental signals from fossil fuel emissions and biospheric sources and sinks. The lower tropospheric CO_2 mean concentrations between 0–4000 m alt were 370.1 ± 4.0 ppm during CAATER-1 (May) and 371.7 ± 5.0 ppm during CAATER 2 (October). Thus, despite a stronger biogenic (biospheric) uptake in Spring, reducing background CO_2 over the whole Northern Hemisphere and CO_2 over the European continent, the lower troposphere mean level in May was roughly similar to October. For CAATER-2, the mean CO concentration was 177 ± 61 ppb.

As a reference for our analysis, we computed marine background concentrations of CO_2 and CO in the boundary layer, called MBL values. These MBL values were computed using records from the Mace Head station that is part of the RAMCES network (https://ramces.lsce.ipsl.fr/). Mace Head is located on the west coast of Ireland, thus, marine background concentrations during CAATER could be inferred by selecting the marine wind sector data averaged over each campaign's duration. For CO_2, the MBL values obtained are 374.5 ± 0.3 ppm during CAATER 1 and 367.9 ± 0.2 ppm during CAATER 2; for CO the MBL value computed for CAATER 2 is 131.1 ± 0.2 ppb.

In order to investigate the origin of the sampled air masses, we computed for each flight, 5-days backtrajectories at different measurement points of the flight path. The HYSPLIT-4 (Hybrid Single-Particle Lagrangian Integrated Trajectory) was used to compute these backtrajectories (Draxler and Hess, 1998). Four-dimensional (x, y, z, t) gridded meteorological fields from NOAA/NCEP (National Centers for Environmental Predictions, http://www.ncep.noaa.gov/) global reanalysis data were used to drive HYSPLIT-4 (analysis every 6 h, $1° \times 1°$ horizontal resolution, 14 vertical levels). Each trajectory was calculated as the time integrated advection of a single particle. The integration time-step can vary during the simulation, as it is computed from the requirement that the advection distance per time-step should be less than 75% of the meteorological grid spacing. This linear integration method is common (e.g. Kreyszig, 1968) and has been used for trajectory analysis (Petterssen, 1940) for quite some time. Advection is computed from the average of the 3-D-velocity vector for the position at time t and the position at time $t-1$. The accuracy of the model has been quantified by testing the model trajectories against balloon data: the difference was about 10 to 20% (Draxler, 1998).
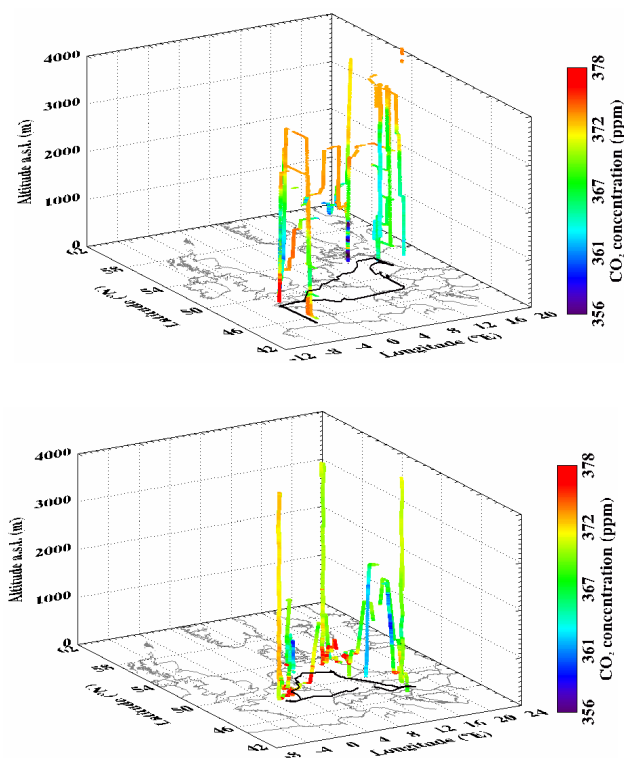

Fig. 4. CO_2 concentration 3-D distribution according to longitude, latitude and altitude. The flight patterns are projected on the longitude/latitude plan. (top: CAATER-1, bottom: CAATER-2).

3.2 Air masses sampled in May 2001 during CAATER-1

Back-trajectories calculated for each flight of CAATER 1 are shown in Fig. 5 (a projection of Fig. 4 for CAATER 1 in the horizontal longitude-latitude plan). About 58% of the air masses sampled came from the north-west, 37% from the north-east and only 5% from the south-east.

On 23 May 2001 (Fig. 5a), between 4° E and 2° W, the back-trajectories indicate a continental origin from the north-east, with air masses being advected in the boundary layer (<2000 m) and carrying low CO_2 values of ≈ 360 ppm. As the aircraft moved west of 2° W, the sampled air mass reached values in the range of 372–375 ppm. Indeed during that day, from ECMWF reanalysis, we know that there was no special feature in the vertical structure of the atmosphere such as convection that can explain this difference in concentration. Backtrajectories show that between 2° E and 2° W, air masses were advected from the east-south-east in the boundary layer, while they were advected from the north-east passing above the ocean between 2° W and 4° W before landing in Brest. It is thus very likely that the depletion of CO_2 observed between 2° E and 2° W on 23 May 2001 was due to advection of air formerly exposed to terrestrial CO_2 uptake. Indeed two days later (see Fig. 5c) we encountered
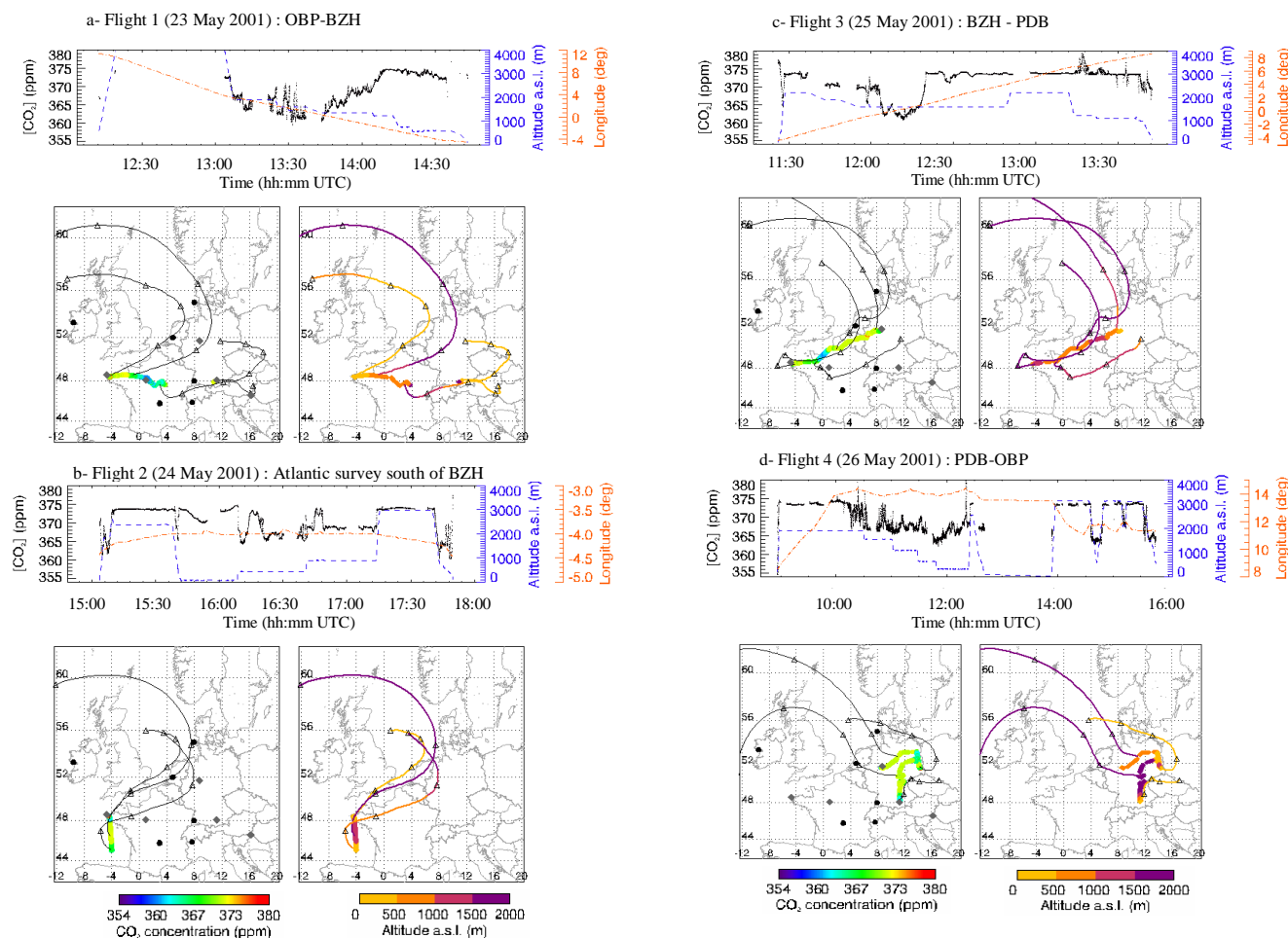
Fig. 5. (a, b) Back-trajectories computed over 96 h for flight 1 and flight 2. The distance between 2 triangles is 24 h. Left panels show CO_2 concentrations along the flight path and back-trajectories. Right panels show the altitude of the flight, and back-trajectories colored according to air mass altitude. Black circles represent ground stations named in Fig. 1. Altitude is given in meters above the sea level (m a.s.l.). Note that some of the back-trajectories are outside the latitude and longitude chosen borders, but these are so diluted that they do not give any relevant information.

Fig. 5. (c, d) Back-trajectories computed over 96 h for flight 3 and flight 4. The distance between 2 triangles is 24 h. Left panels show CO_2 concentrations along the flight path and back-trajectories. Right panels show the altitude of the flight, and back-trajectories colored according to air mass altitude. Black circles represent ground stations named in Fig. 1. Altitude is given in meters above the sea level (m a.s.l.). Note that some of the back-trajectories are outside the latitude and longitude chosen borders, but these are so diluted that they do not give any relevant information.

a similar CO_2 depletion between 2° E and 2° W, also below 2000 m, around midday and with similar pressure and wind conditions than on 23 May 2001. For this flight, simultaneous in-situ CO_2 and ^{222}Rn measurements allowed us to identify the role of terrestrial CO_2 uptake over France at that period (Xueref-Remy et al., 2011, Part 2). Between 2° W and 4° W, we can conclude from the HYSPLIT backtrajectories that an oceanic air mass was sampled, whose CO_2 concentration was close to the MBL value defined in Sect. 3.1 (374.5 ppm).

On 24 May 2001 (Fig. 5b) over the Bay of Biscay, air masses were influenced by local anthropogenic emissions near the surface close to BZH (∼378 ppm). The aircraft flight

over the Bay of Biscay first sampled air advected from the English Channel at ≈4000 m alt with oceanic CO_2 concentrations of 372–374 ppm, and then continental air from northeastern Europe, with CO_2 depleted by plant uptake down to 360 ppm.

On 25 May 2001 (Fig. 5c), the air mass was first oceanic (374 ppm). Moving eastwards between 3° W and 1° E, sampled continental air masses gave CO_2 concentrations of approximately 360 ppm (biospheric-influenced values, that are similar to those sampled during 23 May on roughly the same route westwards: see above), then oceanic air, followed again by anthropogenic emission plumes over the Ruhr area with $CO_2 \sim 380$ ppm. The signal of this high emission region of

Europe when compared to the "biospheric" minimum further east is of the order of 20 ppm in the whole boundary layer.

On 26 May 2001 (Fig. 5d), we sampled oceanic, biospheric and anthropogenic air masses. Around 12° E in the mid-afternoon, we measured low concentrations (around 365 ppm). The easterly flow associated with these minimum CO$_2$ values corresponds to air masses advected into the boundary layer, and thus directly exposed to continuous biospheric uptake. In contrast around 14° E, an air mass coming from the west and north-west was sampled. Back trajectories indicated that this air mass is exposed to anthropogenic emissions, and contains CO$_2$ values 25 ppm above these low concentrations. Note that all these measurements were recorded in the PBL at altitudes lower than 400 m a.s.l.; backtrajectories show that the high-CO$_2$ air mass sampled at 14° E was advected from the north-west at altitudes below 500 m, with an origin that can be approximately traced to anthropogenic emissions over Northern Germany and Denmark. On the other hand, air masses coming from altitudes higher than 1700 m from the West, with tropospheric air decoupled from surface fluxes, are associated to CO$_2$ concentrations (~374 ppm) close to the marine background value defined in Sect. 3.1 (374.5 ppm).

3.3 Air masses sampled in October 2002 during CAATER-2

We also analyze the relationship between CO and CO$_2$ observed during the CAATER 2 campaign (unfortunately, no CO data is available for CAATER 1). In air masses influenced by combustion processes, we expect a positive correlation between the residual concentrations of CO and CO$_2$ computed to background concentrations. This should enable the identification of fossil fuel CO$_2$ in total CO$_2$ in sampled air masses (e.g. Levin and Karstens, 2007). This (too) simple theory is however complicated by (1) different ratios of CO to fossil fuel CO$_2$ emissions in the various types of combustion, (2) mixing of air rich in fossil fuel CO$_2$ with oceanic or vegetation fluxes, a process that changes CO$_2$ without changing CO, and (3) chemical production of secondary CO from biogenic volatile organic compounds, which in summer can contribute as much CO as anthropogenic combustions (Rivier et al., 2006); this process tends to increase CO but not CO$_2$. During the CAATER-2 campaign, these three processes (different mix of combustion, mix of oceanic, vegetation and fossil fuel CO$_2$, secondary CO production) are unfortunately at work simultaneously. This, in principle, makes the inferrence of fossil fuel CO$_2$ very difficult, as already noted when using ground-based station records (Karstens et al., 2006; Levin et al., 2007). In this context, it is interesting to check the relationship between CO and CO$_2$ in the diverse sampled air masses during the CAATER-2 campaign (see Sect. 3).

First, we identified the different air masses in the CAATER-2 dataset classified by their origins (Fig. 6). Then
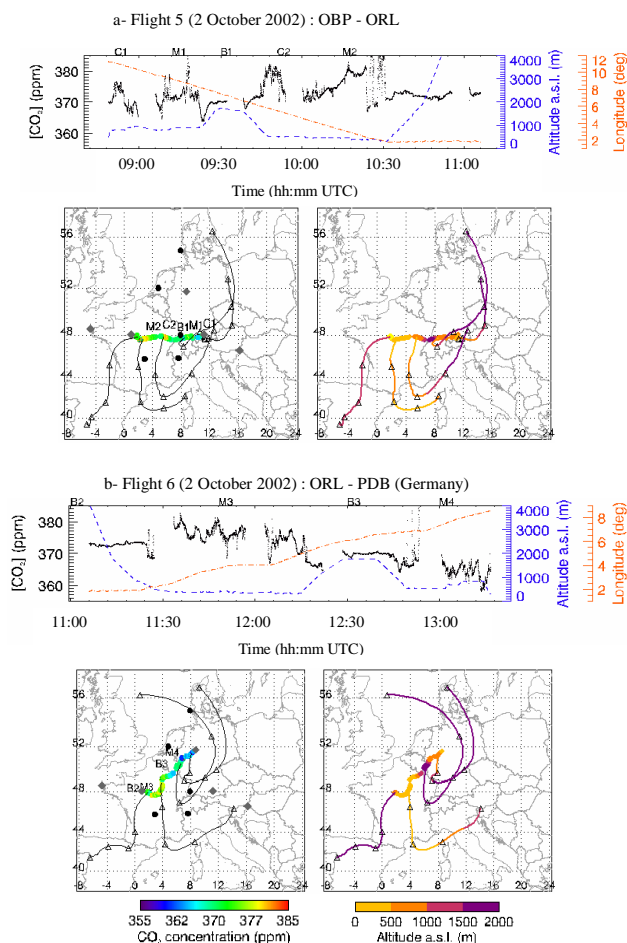

Fig. 6. (a, b) Back-trajectories computed over 96 h for flights 5 and 6. The distance between 2 triangles is 24 h. Left panels show CO$_2$ concentrations along the flight path and back-trajectories. Right panels show the altitude of the flight, and back-trajectories colored according to air mass altitude. Black circles represent ground stations named in Fig. 1. Altitude is given in meters above the sea level (m a.s.l.). Note that some of the back-trajectories are outside the latitude and longitude chosen borders, but these are so diluted that they do not give any relevant information.

we computed the linear regression correlation (R^2 determination factor) and the slope (S) of ΔCO vs. ΔCO$_2$ (delta standing for the difference of the observed concentration to the marine background concentration) for each air mass. The results are presented in Fig. 8. The R^2 and slope values showed a wide range of variation when all air masses are considered without distinction (Table 5). To all R^2, we computed the associated p-value (Table 5): in all cases the correlation significance is higher than 99%.

On 3 October 2002, during the flight from OBP to SOB (Table 2; Fig. 6c) a vertical profile was sampled over a rural location in the Thüringen area (event B4 in Fig. 7). This profile shows CO$_2$ and CO values close to background. The same tropospheric values at 4000 m as those measured
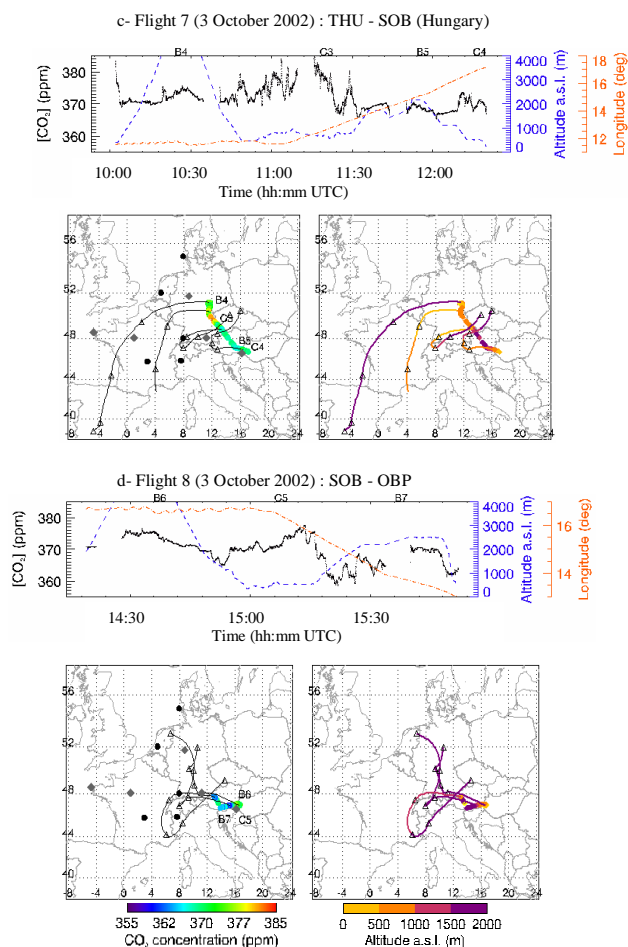
c- Flight 7 (3 October 2002) : THU - SOB (Hungary)

d- Flight 8 (3 October 2002) : SOB - OBP

Fig. 6. (c, d) Back-trajectories computed over 96 h for flights 7 and 8. The distance between 2 triangles is 24 h. Left panels show CO_2 concentrations along the flight path and back-trajectories. Right panels show the altitude of the flight, and back-trajectories colored according to air mass altitude. Black circles represent ground stations named in Fig. 1. Altitude is given in meters above the sea level (m a.s.l.). Note that some of the back-trajectories are outside the latitude and longitude chosen borders, but these are so diluted that they do not give any relevant information.

one day earlier over ORL shows that the signal of sources and sinks is mainly confined to the boundary layer during the CAATER-2 campaign, because of anticyclonic conditions and reduced mixing. An anthropogenic emission plume (event C3 in Fig. 7) was sampled between 12° and 13.5° E, with a small positive ΔCO vs. ΔCO_2 correlation ($R^2 = 0.26$, slope = 1.78 ppb CO ppm^{-1} CO_2). In this C3 event, the origin of the air masses was traced to the high emission Ruhr industrial region. At longitude 17° E (event C4 in Fig. 7) we encountered a better-defined anthropogenic emission plume ($R^2 = 0.47$, slope = 3.2 ppb CO ppm^{-1} CO_2) during the vertical profile over the tall tower of Hegyatsall.
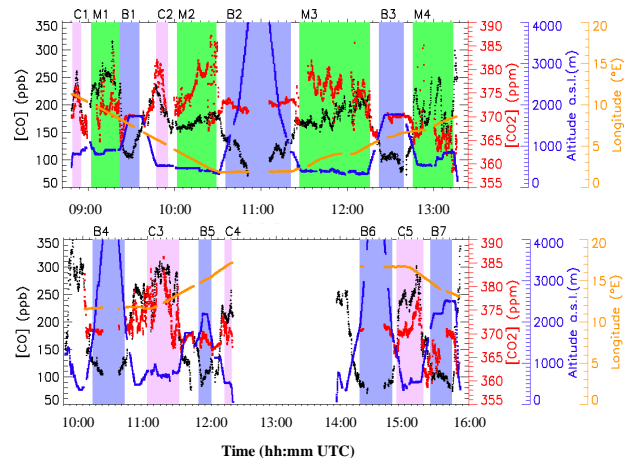

Fig. 7. CO, CO_2 and altitude time series during the CAATER 2 flights (top: 2 October 2002; bottom: 3 October 2002). Striking events have been selected with colorbars (pink is for C: high CO and CO_2 correlation level events, green is for M: mixed determination factor events, blue is for B: tropospheric background events).
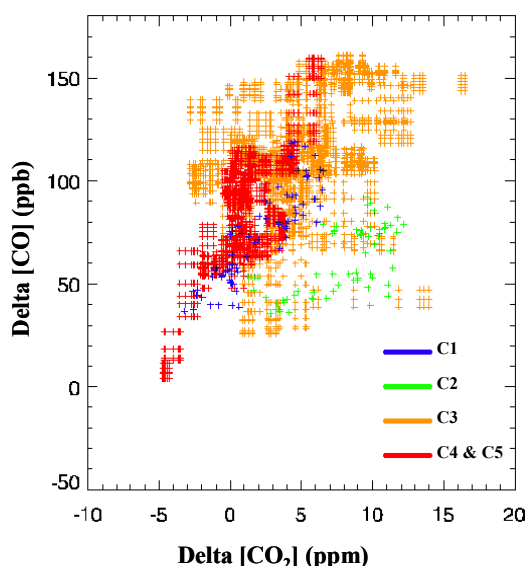
On 3 October 2002, during the (return) flight from SOB to OBP (Fig. 6d), the aircraft climbed above 4000 m (event B6). Background values of CO, CO_2 at 4000 m were checked and confirmed to be unchanged from the flight above the Orleans forest (event B2). Then, an horizontal route was followed in the boundary layer (mean altitude 300 m; event C5 in Fig. 7). Near-surface anthropogenic emission plume sampled west of Hegyhatsal with a high ΔCO vs. ΔCO_2 correlation ($R^2 = 0.88$, slope = 10.37 ppb CO ppm^{-1} CO_2) was most likely of local origin, from Graz (second largest city in Austria with 300 000 people and an international airport). Finally, the airplane crossed Eastern Germany westwards to OBP at 2200 m altitude. Surprisingly low CO_2 values for the month of October (360 ppm) were observed during that last flight, as well as low CO values (110 ppb). The back-trajectories of this flight show a complex pattern, with some air coming from the Alps before reaching the aircraft position.

4   Comparison of CAATER observations to CO:CO$_2$ emission ratios from inventories for anthropogenic-influenced air masses

We selected here only the well-identified anthropogenic-influenced air masses diagnosed from back-trajectories (events C1 to C5). These air masses all show high R^2 values (0.33 to 0.88), but their slope varies from 2.42 to 10.37 ppb CO ppm^{-1} CO_2 (Table 5). These slope values are compared below to the CO:CO$_2$ slope (ρ in kt CO Mt^{-1} CO_2) given by emission inventories (EMEP, 2008) for the region of influence of each air mass.

Table 5. Evaluation of the correlation level between CO_2 and CO for the different events selected from Fig. 7. Each event has been attributed to a class according to its back-trajectory location and direction (from Fig. 6) as explained in the text.

Event	Determination factor R^2	p-value (number of pairs)	Slope $\Delta CO/\Delta CO_2$ (in ppb CO ppm^{-1} CO_2)	Day (in October 2002)
C1	0.82	3.60×10^{-42} ($n = 60$)	6.38	2
C2	0.65	3.14×10^{-39} ($n = 66$)	3.52	2
C3	0.26	0. ($n = 1673$)	1.78	3
C4	0.47	0. ($n = 530$)	3.2	3
C5	0.69	0. ($n = 1461$)	8.93	3
M1	0.13	0. ($n = 141$)	0.9	2
M2	0.35	0. ($n = 2198$)	0.76	2
M3	-0.42	0. ($n = 2968$)	-2.88	2
M4	-0.06	9.11×10^{-3} ($n = 1848$)	-0.36	2
B1	-0.67	1.75×10^{-5} ($n = 100$)	-11.4	2
B2	0.54	0. ($n = 2234$)	12.1	2
B3	-0.41	0. ($n = 886$)	-10.1	2
B4	0.15	6.67×10^{-6} ($n = 922$)	3.56	3
B5	-0.56	0. ($n = 861$)	-7.15	3
B6	-0.43	0. ($n = 556$)	-2.56	3
B7	-0.73	0. ($n = 915$)	-2.36	3

Fig. 8. ΔCO (i.e. CO minus CO marine background concentration) versus ΔCO_2 (i.e. CO_2 minus CO_2 marine background concentration) for the CAATER 2 flights. Colors represent correlated events C1 to C5 as defined in the text. See Sect. 3 for marine background concentration definition.

Air mass C1 was exposed to fossil fuel emission fluxes in Eastern Germany/Western Poland/Southern Sweden (see Sect. 3). It has the highest R^2 (0.82), and a slope $S = 6.38$ ppb CO ppm^{-1} CO_2 higher than the mean inventory derived slope for Germany ($\rho = 5.1$ kt CO/Mt CO_2). One can

see in Fig. 6a that C1 is not only influenced by Eastern Germany, but also by industrial regions (Malmö) in Southern Sweden and in Western Poland, where the CO:CO_2 emission ratio are higher regionally (range 11.1 to 12 kt CO/Mt CO_2).

Air mass C2 was exposed to Rhone valley emissions as well as to CO_2 uptake by vegetation in that region (Sect. 3; see also Fig. 1 (NEE) and the high NDVI values in Fig. A1). This air mass shows a weak $\Delta CO_2 - \Delta CO$ correlation ($R^2 = 0.65$) and a lower slope (3.52 ppb CO ppm^{-1} CO_2) than would be expected from fossil fuel addition alone (France CO:CO_2 emission inventory ratio $\rho = 14$ kt CO/Mt CO_2), indicating a strong biospheric contribution reducing CO_2 while leaving CO unaffected.

Air mass C3, sampled at ~ 900 m, was exposed to emissions in Western Germany from the Ruhr region (Fig. 6c). The R^2 factor is not very high (0.26) and the slope, $S = 1.78$ ppb CO ppm^{-1} CO_2, is quite low compared to the slope of 5.1 kt CO/Mt CO_2 from the emission inventory ratio for Germany, meaning that these emissions have probably been diluted.

Air mass C4, sampled at low altitude (~ 400 m), showed exposure to fossil fuel fluxes in Austria and Czech Republic (Fig. 6c). The mean observed slope is 3.2 ppb CO ppm^{-1} CO_2, close to the emission inventory ratio value for Czech Republic (4.4 kt CO/Mt CO_2), but less close to the one for Austria (10.4 kt CO/Mt CO_2). Thus, fossil fuel CO_2 from Czech Republic must have had a dominant influence on these air masses. However, the large scattering around the linear regression line ($R^2 = 0.47$) indicates interplay of combustion sources with different ratios.

Air mass C5 was sampled at quite low altitude (∼400 m) over rural west Hungary. It was influenced by fluxes from West Hungary (local sources), as well from Austria, Switzerland and Southern Germany (remote sources). Despite the rather complex spiraling back-trajectories shown in Fig. 6d for C5, this air mass keeps a tight positive correlation between ΔCO and ΔCO_2 ($R^2 = 0.69$) and the measured slope (8.93 ppb CO ppm^{-1} CO_2) is close to the regional inventory ratios (Hungary, Austria and Switzerland: $\rho = 10.1$, 10.4 and 8.3 kt CO/Mt CO_2, respectively).

In summary, this analysis shows that despite mixing of fossil fuel CO_2 fluxes with biospheric CO_2 fluxes (which can be >0 in the northern part of Europe and <0 in its southern part; Fig. 1), and spatial and temporal variability in the CO:CO_2 fossil fuel combustion ratios in the different countries (reflecting different reliances on fossil fuel for energy production), it is still possible to use the observed ΔCO:ΔCO_2 slope in atmospheric measurements to quantify the contribution of fossil among other sources of CO_2 a few days/hundreds of km distant from the original source. Here the integrative properties of synoptic atmospheric transport help to average the contrasted CO:CO_2 ratios of local emissions.

5   Comparison of aircraft measurements with surface station measurements

Here we compare the aircraft-measured CO_2 distribution with ground-based station records. The goal is to produce a consistent 3-D picture of the CO_2 field, and to analyze the reasons for concentration differences between altitude and ground level. We used available CO_2 data from several ground-based observatories taken at the time of the campaigns (CBW, PUY, CMN and PRS for CAATER-1; WES, HUN, SCH, PUY, CMN and PRS for CAATER-2; described in Table 3). Hourly data from the stations were selected from 12:00:00 to 18:00:00 h UTC to filter out night-time and morning data, not representative of regional-scale conditions. Indeed in the morning, most of the time, the PBL is growing and encroaches air from aloft while loosing CO_2 accumulated by respiration the former night (Gibert et al., 2007), making CO_2 concentrations more variable. The PBL gets well-mixed and reaches to a relatively stable height only around midday. The footprint of the stations is thus better defined with afternoon values, and more adapted to do a comparison with aircraft data.

Figure 9 provides a projection of Fig. 4 on the vertical longitude/altitude plan. It has been interpolated to produce vertical cross-sections in Fig. 10. For interpolation, the 1 Hz data are first averaged into bins of 100 m altitude. Then a Delaunay triangulation in the altitude, longitude plane was applied (function TRIANGULATE of IDL package). After triangulation, the values were interpolated onto a regular grid (function TRIGRID of IDL package) at resolutions of
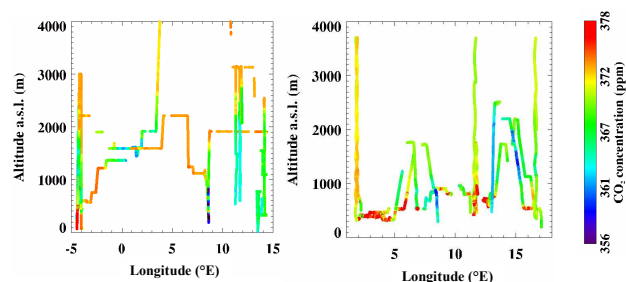

Fig. 9. CO_2 concentrations along the flight patterns represented in function of longitude and altitude during the CAATER 1 (left) and CAATER 2 (right) campaigns.
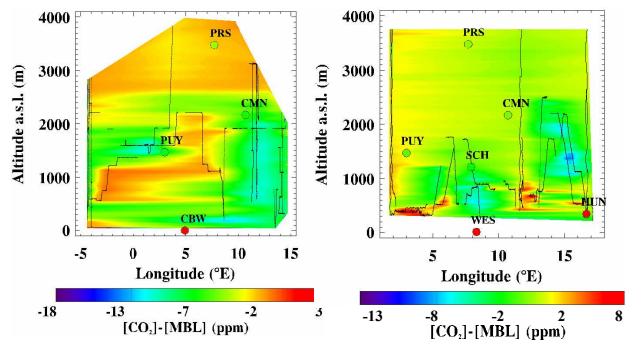

Fig. 10. Interpolation of the CO_2 concentrations for the whole campaign and for each leg according to longitude and altitude during the CAATER 1 (left) and CAATER 2 (right) campaigns. The concentration scale refers to the MBL background concentration of each campaign, as defined in the text. Flight paths are shown in black. Ground station concentrations, averaged in Sect. 1, are shown at the respective station coordinates. Note that for plot convenience, HUN and WES stations during CAATER 2 are shown as being at the maximum of the chosen concentration scale, while indeed they show even higher concentrations (respectively: 12.7 ppm and 38.5 ppm above the marine background concentration, defined in Sect. 3).

200 km horizontally and 100 m vertically. In Fig. 10, the marine background value (reminder: 374.5 ppm for CAATER-1; 367.9 ppm for CAATER-2) was removed from all the data. Figure 11 shows a comparison between ground station values and the mean profile recorded during each campaign. The CO_2 vertical distributions and cross-sections (Figs. 9 and 10) show a large range in the PBL (354 ppm to 378 ppm for CAATER-1; 358 ppm to 378 ppm for CAATER-2) and more homogeneous values in the FT (372 ppm to 374 ppm for CAATER-1; 367 ppm to 373 ppm for CAATER-2). This is true for both campaigns but even more so for CAATER-1 than CAATER-2 (Fig. 11). Figure 10 shows that CO_2 in the CAATER-1 domain is globally below the MBL value (374.5 ppm), whereas it is above the MBL background curve during CAATER-2 (367.9 ppm). One can also observe that CO_2 measured at the CARBOEUROPE stations
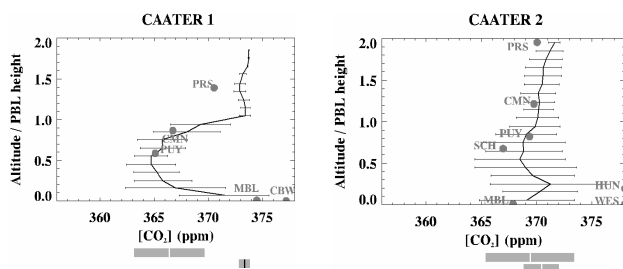
Fig. 11. Variability observed in the PBL and the FT during each campaigns (left: CAATER 1, right: CAATER 2) using profiles only. The altitude of each individual profile has been normalized to the relevant PBL height. The plot shows the mean and standard deviation (1-σ) of CO_2 concentration over layer of 1/10th of the PBL height. The global mean and variability ($\pm$1-σ standard deviation) in the PBL (upper grey bar) and FT (lower grey bar) are shown according to the CO_2 concentration scale of the plot.

CMN agrees better with the aircraft observations than the other stations do, even if it is located outside the campaign domain. CO_2 at CMN (2165 m) compares within 0.7 ppm (0.3 ppm) to the CAATER-1 (CAATER-2) interpolated data for the station's location. During CAATER-1 (May 2001), the high amplitude of the diurnal cycle of CO_2 at CMN (http://gaw.kishou.go.jp/wdcgg/products/cd-rom/cd_14/A/metadata/co2/data/200612120073.html) revealed that this station lay within the PBL. However, as CMN is located at a relatively high altitude and far from local anthropogenic sources, during CAATER-2 it was now located in the free troposphere. It was measuring similar air masses from the West as those recorded by the aircraft during the closest profile (around 12° E), on which the interpolation at CMN mainly relies. Interestingly, at PRS (4000 m) which was located in the free troposphere during both campaigns, interpolated airborne data and station observations are different by about 3 ppm and 0.5 ppm for CAATER-1 and CAATER-2, respectively. Indeed, the CAATER-1 interpolation lies on one profile done above northern Germany with air masses coming from the north (Fig. 5) while PRS is located further south, sampling air masses from the south, east and west as it can be seen on Fig. 5. This reveals a gradient of a few ppm in the free troposphere over Western Europe.

CO_2 measurements at surface stations CBW and WES are influenced by large nearby urban emissions from the Amsterdam urban area and Northern German cities, which diffuse with altitude and so differ significantly from aircraft observations. CO_2 at CBW and WES (respectively WES and HUN) was more than 4 ppm higher (respectively 11 ppm) than the PBL value sampled by the aircraft during CAATER-1 (respectively during CAATER-2).

Both PUY and SCH stations are located on the top of mid-elevation mountains (1205 m alt and 1465 m alt respectively for SCH and PUY) over urbanized valleys. During the morning and early afternoon, in spring and summer, SCH receives air advected by up-slope winds, bringing anthropogenic emissions from valleys that have accumulated during the night; and in the late afternoon, air is cleared of this local influence on windy days (Schmidt et al., 2001). Therefore, CO_2 concentrations at SCH averaged between 12:00 UTC and 18:00 UTC and are less contaminated, but not exempt from urban emissions from the Ruhr region cities. Station data match CAATER-2 campaign aircraft data very well (no data was available during CAATER-1). At PUY, local mesoscale circulations can either bring emission plumes from Clermont-Ferrand, or air from rural areas, depending on wind direction. Both at SCH and PUY, the mixing of surface air with tropospheric air masses is always present, explaining why CO_2 values at these stations are between the PBL and the FT (Fig. 10).

6 Analysis of the vertical variability

The CO_2 gradient between the boundary layer and the free troposphere is a key parameter to optimize fluxes using inverse methods. For each profile, the PBL height was determined as the altitude at which the vertical gradient of the potential temperature begins to decrease, and where CO_2 and H_2O present step changes (Gerbig et al., 2003; Ramonet et al., 2002).

To illustrate the CO_2 vertical variability, the altitude of each single profile was then normalized versus the PBL height; the normalized profiles are shown on Fig. 12 for CAATER-1 and Fig. 13 for CAATER-2. To improve readability, data have been averaged over 50 m layers.

As already noticed in the previous section, CO_2 values show a strong variability in the PBL compared to the FT. The mean and standard deviation (std) computed on all data within the PBL are, respectively, 369.9 ppm and 4.0 ppm during CAATER-1; 371.5 ppm and 5.7 ppm during CAATER-2. In the FT, these values are 373.6 ppm and 0.5 ppm for CAATER-1; 371.2 ppm and 1.1 ppm for CAATER-2. In other terms, the atmospheric CO_2 variability over Europe is at least 5 to 8 ppm higher in the PBL than in the FT.

The PBL variability was higher during Spring 2001 than during Fall 2002. Interestingly, the mean CO_2 jump is 3.7 ppm during CAATER-1 and −0.3 ppm during CAATER-2, with a similar FT averaged CO_2 concentration. Also, the mean profile during CAATER-1 shows a minimum in the mid PBL which is not present in in the CAATER-2 mean profile. These 2 points are the result of a higher photosynthetic activity in Spring than in Autumn.

To go deeper into the variability analysis, all individual profiles have been plotted and colored in Figures 12 and 13 according to the location they were recorded in and the origin of the air masses, deduced from backplumes obtained with the LMDZ model and described in the companion paper (Xueref-Remy et al., 2011).

For CAATER 1 (Fig. 12), the CO_2 concentration range is very large in the bottom half of the PBL (355 to 378 ppm), with highest CO_2 values in the Brittany region due to local anthropogenic emissions from the Brest city area, and lowest values in Northern Germany with air depleted by photosynthetic activity. In Southern and Eastern Germany, vegetation seems less active but the signal does not contain urban emissions. In the mid-troposphere, profiles recorded in Brittany come from air masses, travelling between the ocean, the English Channel and rural regions in North-Western France. CO_2 concentrations range between 362 and 368 ppm, depending on the relative importance of continental air masses depleted by photosynthetic activity compared to oceanic air masses. In the FT, the atmosphere does not interact as much with ground sources and sinks, and the signal is therefore constant.

For CAATER 2 (Fig. 13), the CO_2 concentration range in the bottom half of the PBL is lower than for CAATER 1 (364 to 381 ppm). The impact of anthropogenic emissions from the Rühr region is visible in profiles recorded near the German-French border. Profiles recorded in East Germany, close to Berlin, also show some local emission plumes. In the mid PBL, no depletion linked to the biospheric activity was observed, a difference with Spring 2001. The signal is quite homogeneous between the mid PBL and the FT. However, there is a striking zonal gradient in the CO_2 mean mid-PBL concentration of about 11 ppm, revealing: (1) a weaker biospheric activity i.e. Autumn starting earlier in Western Europe than in Eastern Europe – however, this hypothesis does not match with the flux maps given in Fig. 1, that indicates on averaged higher fluxes in the East than in the West of Europe. Also, it does not fit with the NDVI maps as well, given in Annexe 1 – ; (2) a greater mixing of continental and oceanic air in the West of Europe; and/or (3) more CO_2 emissions in the west of Europe such as in France than in the eastern part. Inventories from UNFCCC (2002) give 403.15 Mt CO_2/yr emitted by France against 863.9 Mt CO_2/yr emitted by Germany which mitigates against this last supposition. On the other hand, inventories for Austria (71.0 Mt CO_2/yr), Hungary (57.7 Mt CO_2/yr), Slovenia (16.3 Mt CO_2/yr), and Croatia (20.9 MtCO_2/yr) as well as likely emissions of the Federal Republic of Yugoslavia and Bosnia-Herzegovinia (no inventories available) make it probable that the total of the emissions from these countries (covered by the red region on Fig. 13) are less than those of France and so support supposition 3. However, fluxes shown on Fig. 1 do not match with this hypothesis. Indeed, from ECMWF reanalysis data, we inferred that some convection activity occured in France on 2 October along the flight path to Orleans: this can explain that the dark-blue profiles are straight, since the air was well-mixed likely containing a mixture of CO_2 biospheric emissions from the ground and CO_2 emissions advected from the Rhone valley (blue footprint on Fig. 13), thus charged in anthropogenic CO_2 (CO in the range of 130–160 ppm). Also, the green profile, recorded above Thüringen is straight.
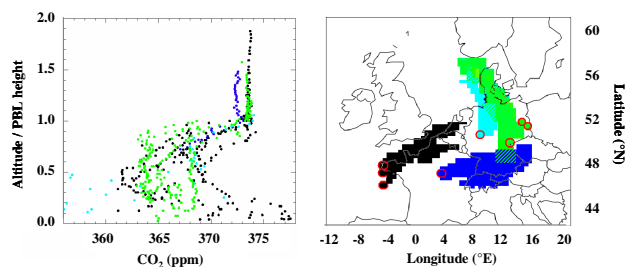

Fig. 12. CAATER 1 vertical variability analysis. Left panel: all CO_2 profiles binned over 50 m layers and standardized to their respective PBL height. Right panel: schema of the regions covered by the back-trajectories of the profiles (profile locations are indicated by circles). Colors of right and left panels correspond.

There was some convection developing in this region, meaning that likely the air was well-mixed and influenced by anthropogenic CO_2 emissions (CO again in the range of 130–160 ppm) as well as a priori less-concentrated CO_2 signals from the biosphere activity advected from Germany (green footprint on Fig.13). The shape of the turquoise profiles and even more of the red profiles is very different, with a marked depletion in the mid-PBL. No convection activity could be identified at these locations and times. The CO signal reaches values as low as 100 ppb, thus, excluding anthropogenic contribution. The air mass footprints are continental (east Germany for the turquoise profiles, Central Europe for the red profiles), excluding as well oceanic signal contribution. It is thus likely, that there was some biospheric sinks still acting in east Germany and even in a stronger manner in Central Europe at that time. Once again, model fluxes do not relate this point, but biospheric fluxes are not always properly modelled as we discuss in the companion paper (Xueref-Remy et al., 2011). It would be interesting in the future to conduct new airborne campaigns to assess if the observed gradient is always present at the fall season, or if it was only punctual. Using tracers such as CO, Radon 222 and carbon isotopes would also help to discriminate the role of anthropogenic, biospheric and oceanic sources and sinks.

7 Conclusions

This paper focuses on atmospheric CO_2 variability observed during the CAATER campaigns that occured above western Europe on 23–26 May 2001 (CAATER 1) and 2–3 October 2002 (CAATER 2) between the ground and 4000 m a.s.l. Although the aircraft paths were slightly different during CAATER-1 and CAATER-2, the campaigns give a good picture of CO_2 concentration variability over Europe during one Spring and one Fall. The instrumentation provided measurements of in situ CO_2 (precision of 0.2 ppm), CO_2 flasks samples (precision of 0.1 ppm), Radon-222 (precision of 30%) during CAATER-1, and in-situ CO (precision of

5 ppb) during CAATER-2. Despite a stronger biogenic uptake in Spring, the lower tropospheric mean level and the mean variability in May (370.1 ± 4.0 ppm) are roughly similar in October (371.7 ± 5.0 ppm). However, this mean value is lower than the marine boundary layer concentration for CAATER-1 (374.5 ppm) and higher for CAATER-2 (the marine background, 367.9 ppm, being more depleted). A back-trajectory analysis shows that during CAATER-1, dominant winds were coming from the north-west, while they were more balanced between the 4 sectors during CAATER-2.

During CAATER-1, the action of the biospheric sink over rural areas produced atmospheric CO$_2$ values as low as 355 ppm, while the emissions from anthropogenic-influenced regions such as Benelux and the Ruhr valley gave atmospheric CO$_2$ concentration levels of about 380 ppm at approx. 1000 m a.s.l. above these regions.

During CAATER-2, CO$_2$ and CO, were recorded simultaneously which helped us to trace fossil fuel emissions. After a classification of air masses according to their origin,we calculated the ΔCO to ΔCO$_2$ ratio (Δ standing for the difference with the marine boundary layer concentration) and selected only well-identified anthropogenic-influenced air masses diagnosed from back-trajectories. The anthropogenic-influenced air masses show high R^2 values ranging from 0.33 to 0.88 and a large range of slopes (2.42 to 10.37 ppb CO ppm^{-1} CO$_2$). Comparing these slopes to the ones from EMEP inventories for Western Europe countries, we have observed that it is possible to distinguish the contribution of fossil fuel combustion from other sources of CO$_2$ even at a distance of a few days or hundreds of kms from the source.

Aircraft data were compared to surface station observations (CBW, PUY, CMN and PRS for CAATER 1; WES, HUN, SCH, PUY, CMN and PRS for CAATER 2). Only afternoon values were selected so as to get data representative of the regional scale. Urban stations such as CBW and WES are strongly influenced by local emissions and were decoupled from the airborne observations. Depending on the time of the day and the meteorological situation, stations on top of small mountains such as SCH and PUY may be located in the boundary layer (PBL) or in the free troposphere (FT); they match the airborne observations if in the FT and not contaminated by air emanating from the valley. Stations when in the FT such as CMN match airborne measurements quite well, as the atmosphere is well mixed at that altitude. However, PRS which is in the FT but a few 100 km further from the aircraft path differs by 3 ppm from the airborne measurements, which highlights the existence of a CO$_2$ gradient of a few ppm above Europe in the FT.

As the gradient between the PBL and the FT is a key parameter for inverse modeling we have also analyzed CO$_2$ vertical variability. The mean jump between the PBL and the FT is of the order of 3.7 ppm during CAATER 1 and -0.3 ppm during CAATER 2, and the variability is at least 5 to 8 times higher in the PBL than in the FT. A strong zonal
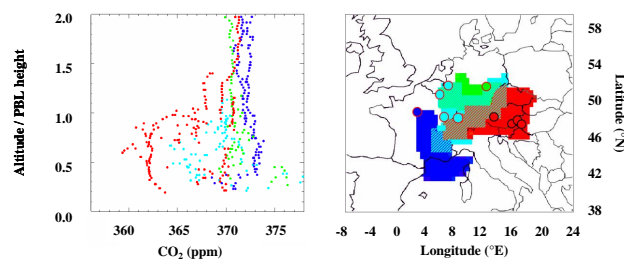

Fig. 13. CAATER 2 vertical variability analysis. Left panel: all CO$_2$ profiles binned over 50 m layers and standardized to their respective PBL height. Right panel: schema of the regions covered by the backplumes associated with the profiles (profile locations are indicated by circles). Colors of right and left panels correspond.

gradient of about 11 ppm in the CO$_2$ mean mid-PBL concentration with higher concentrations in the west during the CAATER 2 campaign is striking. This gradient could originate from a transport effect (a better mixing in Western Europe), an earlier Autumn in the west compared to the east, or higher emissions from Western Europe than Eastern Europe. To better understand this gradient and discriminate correctly beween these hypotheses, more airborne vertical profiles are needed. Such a program has been undertaken in the framework of the CARBOEUROPE-IP project in 5 sites (Griffith, Scotland; Orleans, France; Hegyhatsal, Hungary; Bialystok, Poland; and La Muela, Spain), with one flight every 5 days. The data are currently being analyzed and future publications are planned. In the companion paper (Xueref-Remy et al., 2011, Part 2) we conduct a comparison of vertical profiles between models and observations. We also attempt to calculate CO$_2$ fluxes during the CAATER 1 campaign using the so-called "Radon method" based on simultaneous CO$_2$ and Radon-222 observations (Schmidt et al., 2003) and modeling tools.

Appendix A

NDVI maps for Western Europe during the CAATER campaigns

These NDVI maps provided by the SPOT VGT-4 satellite system give us information on the photosynthetic activity. They clearly show a higher photosynthetic activity during Spring 2001 than during Fall 2002 in Western Europe.
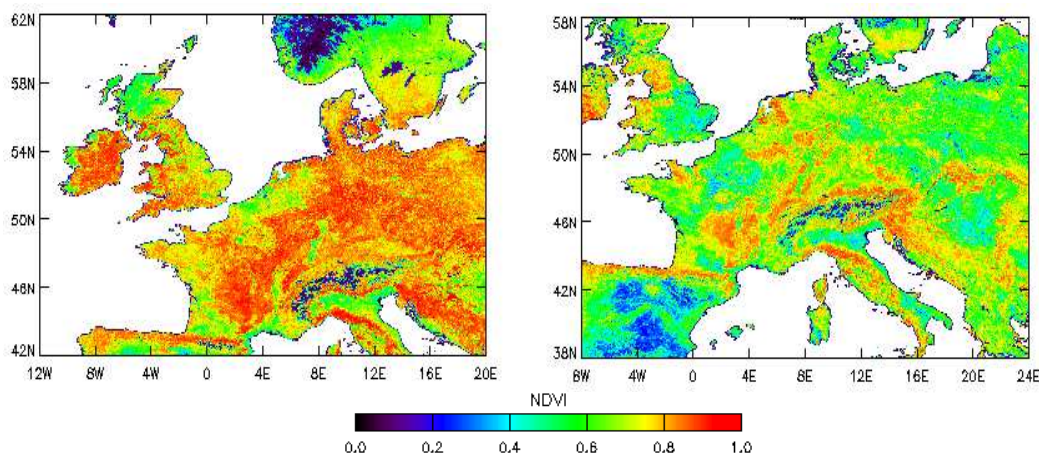
Fig. A1. NDVI maps on 21 May 2001 for CAATER 1 (left) and on 1 October 2002 for CAATER 2 (right).
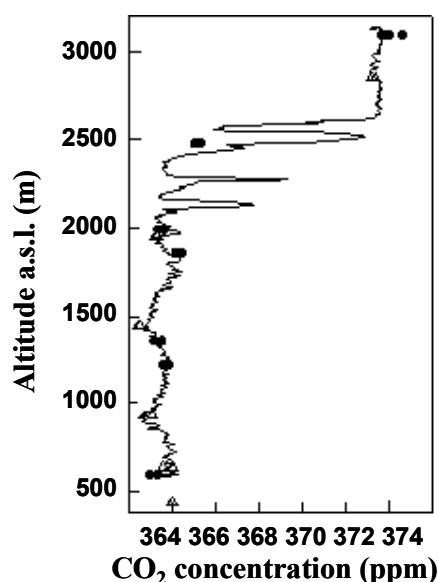

Fig. B1. Coordinated flights over Thringen on 26 May 2001 at 14:30:00 h UTC (in situ: plain line, LSCE flasks: plain circles; Jena flasks: open triangles).

Appendix B

Validation of the CO_2 in situ analyser

As explained in Sect. 2, flask measurements were compared to CONDOR measurements. We show here (Fig. B1) a comparison for 26 May 2001 over Thüringen at 14:30:00 h UTC, during which the Falcon flight was co-ordinated with those of a small aircraft equipped with a flask sampler from the MPI-BGC Jena group. LSCE flasks (circles), Jena flasks (triangles) and CONDOR (plain line) data agree within 0.2 ppm.

References

Andres, R.J., Marland, G., Fung, I., and Matthews, E.: A $1° \times 1°$ distribution of carbon dioxide emissions from fossil fuel consumption and cement manufacture 1950–1990, Global Biogeochem. Cy., 10, 419–429, 1996.

Baker, D. F., Doney, S. C., and Schimel, D. S.: Variational data assimilation for atmospheric CO_2, Tellus B, 58(5), 359–365, 2006.

Carouge, C., Bousquet, P., Peylin, P., Rayner, P. J., and Ciais, P.: What can we learn from European continuous atmospheric CO_2 measurements to quantify regional fluxes – Part 1: Potential of the 2001 network, Atmos. Chem. Phys., 10, 3107–3117, doi:10.5194/acp-10-3107-2010, 2010a.

Carouge, C., Rayner, P. J., Peylin, P., Bousquet, P., Chevallier, F., and Ciais, P.: What can we learn from European continuous atmospheric CO$_2$ measurements to quantify regional fluxes – Part 2: Sensitivity of flux accuracy to inverse setup, Atmos. Chem. Phys., 10, 3119–3129, doi:10.5194/acp-10-3119-2010, 2010b.

Drexler, R. R. and Hess, G. D.: An overview of the Hysplit 4 modelling system for trajectories, dispersion, and deposition, Austral. Met. Mag., 47, 295–308, 1998.

EMEP: Greenhouse gas emission trends and projections in Europe 2008, ISBN: 978-92-9167-981-2, vol. 5, 2008

Filippi, D., Le Roulley, J. C., Ramonet, M., and Ciais, P.: Comprehensive greenhouse gases and radon profilings over Europe, 6th international Conference on CO$_2$, Sendai, Japan, October 2002, 2002.

Geels, C., Gloor, M., Ciais, P., Bousquet, P., Peylin, P., Vermeulen, A. T., Dargaville, R., Aalto, T., Brandt, J., Christensen, J. H., Frohn, L. M., Haszpra, L., Karstens, U., Rödenbeck, C., Ramonet, M., Carboni, G., and Santaguida, R.: Comparing atmospheric transport models for future regional inversions over Europe – Part 1: mapping the atmospheric CO2 signals, Atmos. Chem. Phys., 7, 3461–3479, doi:10.5194/acp-7-3461-2007, 2007.

Gerbig, C., Lin, J. C., Wofsy, S. C., Daube, B. C., Andrews, A. E., Stephens, B. B., Bakwin, P. S., and Grainger, C. A.: Towards constraining regional-scale fluxes of CO$_2$ with atmospheric observations over a continent: 1. Observed Spatial Variability, J. Geophys. Res., 108, 4756, doi:10.1029/2002JD003018, 2003.

Gloor, M., Fan, S.-M., Pacala, S., and Sarmiento, J.: Optimal sampling of the atmosphere for purpose of inverse modelling – a model study, Global Biogeochem. Cy., 14(1), 407–428, 2000.

Gurney, K. R., Law, R. M., Denning, A. S., Rayner, P. J., Baker, D., Bousquet, P., Bruhwiler, L., Chen, Y. H., Ciais, P., Fan, S., Fung, I. Y., Gloor, M., Heimann, M., Higuchi, K., John, J., Kowalczyk, E., Maki, T., Maksyutov, S., Peylin, P., Prather, M., Pak, B. C., Sarmiento, J., Taguchi, S., Takahashi, T., and Yuen, C. W.: TransCom 3 CO$_2$ inversion intercomparison: 1. Annual mean control results and sensitivity to transport and prior flux information, Tellus, 55B(2), 555–579, 2003.

Gurney, K. R., Law, R. M., Denning, A. S., Rayner, P. J., Pak, B. C., Baker, D., Bousquet, P., Bruhwiler, L., Chen, Y.-H., Ciais, P., Fung, I. Y., Heimann, M., John, J., Maki, T., Maksyutov, S., Peylin, P., Prather, M., and Taguchi, S.: Transcom 3 inversion intercomparison: Model mean results for the estimation of seasonal carbon sources and sinks, Global Biogeochem. Cy., 18, GB1010, doi:10.1029/2003GB002111, 2004.

Intergovernmental Panel on Climate Change: IPCC Climate Change 2007: The Scientific Basis, Cambridge Univ. Press, New York, 2007.

Karstens, U., Gloor, M., Heimann, M., and Rödenbeck, C.: Insights from simulations with high-resolution transport and process models on sampling of the atmosphere for constraining mid-latitude land carbon sinks, J. Geophys. Res., 111, D12301, doi:10.1029/2005JD006278, 2006.

Krinner, G., Viovy, N., De Noblet-Ducoudré, N., Ogée, J., Polcher, J., Friedlingstein, P., Ciais, P., Sitch, S., and Prentice, I. C.: A dynamic global vegetation model for studies of the coupled atmosphere-biosphere system, Global Biogeochem. Cy., 19, GB1015, doi:10.1029/2003GB002199, 2005.

Kreyszig, E.: Advanced engineering mathematics, 2nd Ed. J. Wiley

and Sons, New York, 898 pp., 1968.

Law, R. M., Peters, W., Rodenbeck, C., and TRANSCOM contributors: TransCom model simulations of hourly atmospheric CO$_2$: experimental overview and diurnal cycle results for 2002, Global Biogeochem. Cy., 22, GB3009, doi:10.1029/2007GB003050, 2008.

Levin, I. and Karstens, U.: Inferring high-resolution fossil fuel CO$_2$ records at continental sites from combined 14CO$_2$ and CO observations, Tellus, 59B, 245–250, doi:10.1111/j.1600-0889.2006.00244.x, 2007.

Nedelec, P., Cammas, J.-P., Thouret, V., Athier, G., Cousin, J.-M., Legrand, C., Abonnel, C., Lecoeur, F., Cayez, G., and Marizy, C.: An improved infrared carbon monoxide analyser for routine measurements aboard commercial Airbus aircraft: technical validation and first scientific results of the MOZAIC III programme, Atmos. Chem. Phys., 3, 1551–1564, doi:10.5194/acp-3-1551-2003, 2003.

Patra, P. K., Law, R. M., Peters, W., Rodenbeck, C., Takigawa, M., Aulagnier, C., Baker, I., Bergmann, D. J., Bousquet, P., Brandt, J., Bruhwiler, L. M. P., Cameron-Smith, P. J., Christensen, J. H., Delage, F., Denning, A. S., Fan, S., Geels, C., Houweling, S., Imasu, R., Karstens, U., Kawa, S. R., Kleist, J., Krol, M. C., Lin, S.-J., Lokupitiya, R., Maki, T., Maksyutov, S., Niwa, Y., Onishi, R., Parazoo, N., Pieterse, G., Rivier, L., Satoh, M., Serrar, S., Taguchi, S., Vautard, R., Vermeulen, A. T., and Zhu, Z.: TransCom model simulations of hourly atmospheric CO$_2$: analysis of synoptic-scale variations for the period 2002–2003, Global Biogeochem. Cy., 22, GB4013, doi:10.1029/2007GB003081, 2008.

Pépin, L., Schmidt, M., Ramonet, M., Worthy, D., and Ciais, P.: A new gas chromatographic experiment to analyze greenhouse gases in flask samples and in ambient air in the region of Saclay, IPSL internal publication no. 13 (available on request), 2001.

Petterssen, S.: Weather analysis and forecasting, McGraw-Hill Book Company, New York, 221-3, 1940.

Ramonet M., Ciais, P., Nepomniachii, I., Sidorov, K., Neubert, R. E. M., Langendörfer, U., Picard, D., Kazan, V., Biraud, S., Gusti, M., Kolle, O., Schulze, E. D., and Lloyd, J.: Three years of aircraft-based trace gas measurements over the Fyodorovskoye southern taiga forest, 300 km north-west of Moscow, Tellus, 54B, 713–734, 2002.

Rivier, L., Ciais, P., Hauglustaine, D. A., Bakwin, P., Bousquet, P., Peylin, P., and Klonecki, A.: Evaluation of SF$_6$, C$_2$Cl$_4$ and CO to approximate fossil fuel CO$_2$ in the Northern Hemisphere using a chemistry transport model, J. Geophys. Res., 111, D16311, doi:10.1029/2005JD006725, 2006.

Schmidt, M., Glatzel-Mattheier, H., Sartorius, H., Worthy, D. E., and Levin, I.: Western European N$_2$O emissions: A top-down approach based on atmospheric observations, J. Geophys. Res., 106(D6), 5507–5516, 2001.

Schmidt, M., Graul, R., Sartorius, H., and Levin, I.: The Schauinsland CO$_2$ record: 30 years of continental observations and their implications for the variability of the European CO$_2$ budget, J. Geophys. Res., 108(D19), 4619–4626, 2003.

Stephens, B. B., Gurney, K. R., Tans, P. P., Sweeney, C., Peters, W., Bruhwiler, L., Ciais, P., Ramonet, M., Bousquet, P., Nakazawa, T., Aoki, S., Machida, T., Inoue, G., Vinnichenko, N., Lloyd, J., Jordan, A., Heimann, M., Shibistova, O., Langenfelds, R. L., Steele, L. P., Francey, R. J., and Denning, A. S.: Weak

Northern and Strong Tropical Land Carbon Uptake from Vertical Profiles of Atmospheric CO_2, Science, 316(5832), 1732–1735, doi:10.1126/science.1137004, 2007.

Takahashi, T., Wanninkhof, R. H., Feely, R. A., Weiss, R. F., Chipman, D. W., Bates, N., Olafson, J., Sabine, C., and Sutherlandm, S. C.: Proceedings of the 2nd International Symposium CO_2 in the oceans, Tsukuba, Japan, 1, 9–15, 1999.

Takahashi, T., Sutherland, S. C., Sweeney, C., Poisson, A., Metzl, N., Tilbrook, B., Bates, N., Wanninkhof, R., Feely, R. A., Sabine, C., Olafsson, J., and Nojiri, Y.: Global Sea-Air CO_2 Flux Based on Climatological Surface Ocean pCO_2, and Seasonal Biological and Temperature Effect, Deep Sea Res. II, 49(9–10), 1601–1622, 2002.

Xueref-Remy, I., Bousquet, P., Carouge, C., Rivier, L., and Ciais, P.: Variability and budget of CO_2 in Europe: analysis of the CAATER airborne campaigns – Part 2: Comparison of CO_2 vertical variability and fluxes between observations and a modeling framework, Atmos. Chem. Phys., 11, 5673–5684, doi:10.5194/acp-11-5673-2011, 2011.